Effective conductivity, dielectric constant, and diffusion coefficient of digitized composite media via first-passage-time equations

Salvatore Torquato[a] and In Chan Kim[b]
Princeton Materials Institute and Department of Civil Engineering & Operations Research, Princeton University, Princeton, New Jersey 08544

Dinko Cule
Princeton Materials Institute, Princeton University, Princeton, New Jersey 08540-5211

(Received 27 July 1998; accepted for publication 26 October 1998)

We generalize the Brownian motion simulation method of Kim and Torquato [J. Appl. Phys. **68**, 3892 (1990)] to compute the effective conductivity, dielectric constant and diffusion coefficient of digitized composite media. This is accomplished by first generalizing the *first-passage-time equations* to treat first-passage regions of arbitrary shape. We then develop the appropriate first-passage-time equations for digitized media: first-passage squares in two dimensions and first-passage cubes in three dimensions. A severe test case to prove the accuracy of the method is the two-phase periodic checkerboard in which conduction, for sufficiently large phase contrasts, is dominated by corners that join two conducting-phase pixels. Conventional numerical techniques (such as finite differences or elements) do not accurately capture the local fields here for reasonable grid resolution and hence lead to inaccurate estimates of the effective conductivity. By contrast, we show that our algorithm yields accurate estimates of the effective conductivity of the periodic checkerboard for widely different phase conductivities. Finally, we illustrate our method by computing the effective conductivity of the random checkerboard for a wide range of volume fractions and several phase contrast ratios. These results always lie within rigorous four-point bounds on the effective conductivity. © *1999 American Institute of Physics.* [S0021-8979(99)04903-8]

I. INTRODUCTION

There now exist a variety of techniques to obtain two- and three-dimensional images of composite materials, including transmission electron microscopy,[1] scanning tunneling electron microscopy,[2] synchrotron based tomography,[3] and confocal microscopy.[4] All of these imaging methods are nonintrusive, leaving the sample intact and unaltered. The digitized representation of the composite medium calls for numerical techniques that can directly simulate the effective transport, electromagnetic, and mechanical properties of the material. In this article, we shall attempt to address this need by formulating a suitable and efficient algorithm to compute the effective electrical (thermal) conductivity of digitized representations of composite materials via Brownian motion simulations. We note that for reasons of mathematical analogy, the algorithm obtained here is applicable to the determination of the effective dielectric constant, magnetic permeability, and diffusion coefficient of digitized media. The effective diffusion coefficient is a special limiting case equivalent to the effective conductivity when one of the phases is perfectly insulating.

Consider a two-phase digitized composite material consisting of pixels (voxels) of conductivity σ_1 and of conductivity σ_2. As the phase contrast increases, conventional numerical techniques, such as finite differences or finite elements, have difficulty in obtaining accurately the local electric fields in the vicinity of corners that join two conducting-phase pixels (voxels) for a reasonable grid resolution (see Sec. IV). Since the effective conductivity of the sample is given by averages of the local fields,[5] this can lead to inaccurate estimates of the effective conductivity of the digitized medium.

Before discussing our new Brownian motion algorithm to compute the effective conductivity of digitized media, it is helpful to first review previous work on Brownian motion methods to compute the effective conductivity of continuum models. It is well established that the effective conductivity σ_e of a d-dimensional disordered heterogeneous medium can be obtained from the long-time behavior of the mean-square displacement $\langle R^2(t)\rangle$ of a Brownian particle diffusing in the system according to the relation:

$$\sigma_e = \left.\frac{\langle R^2(t)\rangle}{2dt}\right|_{t\to\infty}, \tag{1.1}$$

where t is the time and angular brackets denote an ensemble average. The detailed zig-zag motion of the random walker can be simulated for finite step sizes to yield the effective conductivity.[6] Each step should be infinitesimally small. In practice, one considers walkers with several different small step sizes and then extrapolates to the zero-step-size limit.

However, the random-walk procedure can be considerably sped up by using the *first-passage-time* technique.[7–9]

[a]Electronic mail: torquato@matter.princeton.edu
[b]Permanent address: School of Mechanical Engineering, Kunsan National University, Miryong-Dong 68, Kunsan, Chonbuk 573-701, Korea.

 © 1999 American Institute of Physics

Here a bounded region surrounds the random walker. The random walker can jump onto the surface of this *first-passage* region in one step, if the probability p to first hit the surface and the associated average time τ are known. Since this jump is equivalent to the accumulation of many small steps, the execution time can be considerably reduced[8] compared to random-walk methods that use very small steps. The probability p and time τ will depend on the local phase configuration and conductivities. For continuum models of composites (e.g., dispersions of particles), it is convenient to choose a spherical shape for the first-passage region since one can determine p and τ analytically. Indeed, when the Brownian particle lies in phase i and away from the two-phase interface, p is trivially uniform over the surface and $\tau = R^2/2d\sigma$,[9] where R is the radius of the first-passage sphere that just touches the nearest multiphase interface, at which point the walker then jumps to a random location on the surface of the first-passage sphere with an average time τ. This step is repeated until the random walker gets very close to the interface. Near the interface, a first-passage sphere is constructed that will encompass both phases. Again, the walker jumps on the sphere surface according to the ''interface'' probability p and time taken τ is recorded. (Kim and Torquato[9] gave explicit expressions for the interface probability p and time τ in one, two, or three dimensions.) This process of constructing first-passage spheres around the Brownian particle is repeated until it has properly sampled the composite; the total time (proportional to the mean square displacement) then gives the effective conductivity when averaged over many random walkers. The effective conductivity of various dispersions of cylinders,[9] spheres,[10] and spheroids[11] have been computed in this way.

For digitized media, it is natural to consider the use of first-passage *squares* in two dimensions and *cubes* in three dimensions. However, unlike the case of spheres, the probability p is not uniform on the square or cube boundary, even in the homogeneous case. Accordingly, the problem can no longer be formulated solely in terms of jumping probabilities but rather in terms of jumping probability density functions. Thus, we must generalize the first-passage-time formalism of Kim and Torquato.[8,9] We shall first do so for first-passage regions of arbitrary shape and then specialize to squares and cubes.

The remainder of the article is organized as follows: In Sec. II, we derive general first-passage-time equations for first-passage regions of arbitrary shape. In Sec. III, we specialize the results of the previous section to digitized media in both two and three dimensions. In Sec. IV, we describe the details of the first-passage-time simulation technique to compute the effective conductivity of digitized composite media. The algorithm is then applied in Sec. V to compute the effective conductivity of periodic and random checkerboards. We make concluding remarks in Sec. VI.

II. GENERAL FIRST-PASSAGE TIME FORMALISM

Here we will generalize previous first-passage-time formalisms for homogeneous media[7–9] and heterogeneous media.[9]

A. Homogeneous situation

Consider a Brownian particle (random walker) diffusing in a d-dimensional homogeneous medium of conductivity σ. At some instant of time, let us surround the particle with a *first-passage region* Ω having a bounding surface $\partial\Omega$. Let $\mathbf{r}$ be the position inside Ω and $\mathbf{r}_B$ be a specific point on the boundary $\partial\Omega$.

We introduce the *canonical function* $P(\mathbf{r},\mathbf{r}_B,t)$ associated with the walker striking or hitting the surface $\partial\Omega$ in the vicinity of $\mathbf{r}_B$ for the *first time* at time t when the walker starts at $\mathbf{r}$. The canonical function $P(\mathbf{r},\mathbf{r}_B,t)$ is a probability density function in the variable $\mathbf{r}_B$ and a cumulative probability distribution function in the time variable t and satisfies the time-dependent diffusion equation

$$\sigma\nabla^2 P(\mathbf{r},\mathbf{r}_B,t)=\frac{\partial}{\partial t}P(\mathbf{r},\mathbf{r}_B,t), \quad \mathbf{r} \text{ in } \Omega, \ t>0, \tag{2.1}$$

subject to the following initial and boundary conditions:

$$P(\mathbf{r},\mathbf{r}_B,t=0)=0, \quad \mathbf{r} \text{ in } \Omega \tag{2.2}$$

$$P(\mathbf{r},\mathbf{r}_B,t)=\delta(\mathbf{r}-\mathbf{r}_B), \quad \mathbf{r} \text{ on } \partial\Omega, \ t>0. \tag{2.3}$$

To our knowledge, the above general description is new and generalizes previous first-passage-time formulations.[7–9] We will use this formalism to derive a well-known result for the cumulative function $C(\mathbf{r},t)$ and what we believe to be a new result for the probability density function $p(\mathbf{r},\mathbf{r}_B)$, all of which are described below.

We desire to find the cumulative probability distribution $C(\mathbf{r},t)$ associated with the walker, starting at $\mathbf{r}$, to first hit any point on the surface $\partial\Omega$ at time t. This can be found by integrating the *canonical function* $P(\mathbf{r},\mathbf{r}_B,t)$ over the boundary, i.e.,

$$C(\mathbf{r},t)=\int_{\partial\Omega} P(\mathbf{r},\mathbf{r}_B,t)\,d\mathbf{r}_B. \tag{2.4}$$

From this expression and relations (2.1)–(2.3), we see that C must satisfy the time-dependent diffusion equation

$$\sigma\nabla^2 C(\mathbf{r},t)=\frac{\partial}{\partial t}C(\mathbf{r},t), \quad \mathbf{r} \text{ in } \Omega, \ t>0, \tag{2.5}$$

subject to the initial and boundary conditions:

$$C(\mathbf{r},t=0)=0, \quad \mathbf{r} \text{ in } \Omega, \tag{2.6}$$

$$C(\mathbf{r},t)=1, \quad \mathbf{r} \text{ on } \partial\Omega, \ t>0. \tag{2.7}$$

These are standard equations in Brownian motion theory.[12] Of course, the derivative $\partial C/\partial t$ is just the associated probability density function.

The *average hitting time* $\tau(\mathbf{r})$ is the first moment of the probability density function, i.e.,

$$\tau(\mathbf{r})=\int_0^\infty t\frac{\partial C}{\partial t}\,dt. \tag{2.8}$$

The quantity τ is the average time taken by the diffusing particle to hit the surface $\partial\Omega$ for the first time when starting

from $\mathbf{r}$. A mean hitting time of concern in simulations is the case when the random walker starts at the origin ($\mathbf{r}=\mathbf{0}$). Henceforth, we will denote this mean hitting time by simply dropping the argument $\mathbf{r}=\mathbf{0}$, i.e.,

$$\tau \equiv \tau(\mathbf{r}=\mathbf{0}). \tag{2.9}$$

We note that in the special case when the first-passage region is a d-dimensional sphere of radius R centered at the origin, then we have the very simple expression[9]

$$\tau = \frac{R^2}{2d\sigma}. \tag{2.10}$$

The mean hitting time $\tau(\mathbf{r})$ is obtained by first solving the time-dependent equation for C [Eqs. (2.5)–(2.7)] and carrying out the time integral indicated in Eq. (2.8). One can obtain an alternative *steady-state* formulation for $\tau(\mathbf{r})$. We begin by taking the Laplacian of the general expression (2.8) for the mean hitting time $\tau(\mathbf{r})$ and using relation (2.5); we find that

$$\begin{aligned}\nabla^2\tau(\mathbf{r}) &= \frac{1}{\sigma}\int_0^\infty t\frac{\partial^2 C}{\partial t^2}dt,\\ &= \frac{1}{\sigma}\int_0^\infty\left\{-\frac{\partial C}{\partial t}+\frac{\partial}{\partial t}\left[t\frac{\partial C}{\partial t}\right]\right\}dt,\\ &= \frac{1}{\sigma}\left[-C\big|_0^\infty + t\frac{\partial C}{\partial t}\bigg|_0^\infty\right].\end{aligned} \tag{2.11}$$

The second line of Eq. (2.11) follows by integration by parts. The second term in the last line of Eq. (2.11) is zero since $\partial C/\partial t$ remains bounded at $t=0$ and tends to zero when $t\to\infty$. Finally, application of the initial and boundary conditions (2.6) and (2.7) in expression (2.11) yields the steady-state diffusion equation

$$\sigma\nabla^2\tau(\mathbf{r}) = -1, \quad \mathbf{r} \text{ in } \Omega, \tag{2.12}$$

subject to the absorbing boundary condition

$$\tau(\mathbf{r}) = 0, \quad \mathbf{r} \text{ on } \partial\Omega. \tag{2.13}$$

We will also need to determine the probability density function $w(\mathbf{r},\mathbf{r}_B)$ associated with hitting the vicinity of a particular position $\mathbf{r}_B$ on the surface $\partial\Omega$ for the first time when the walker starts at $\mathbf{r}$. This is obtained by integrating the canonical probability density function $\partial P(\mathbf{r},\mathbf{r}_B,t)/\partial t$ over all times, i.e.,

$$\begin{aligned}w(\mathbf{r},\mathbf{r}_B) &= \int_0^\infty \frac{\partial P}{\partial t}dt,\\ &= P(\mathbf{r},\mathbf{r}_B,t=\infty).\end{aligned} \tag{2.14}$$

This expression in conjunction with relations (2.1)–(2.3) yields the Laplace equation

$$\nabla^2 w(\mathbf{r},\mathbf{r}_B) = 0, \quad \mathbf{r} \text{ in } \Omega, \tag{2.15}$$

subject to the boundary condition

$$w(\mathbf{r},\mathbf{r}_B) = \delta(\mathbf{r}-\mathbf{r}_B). \tag{2.16}$$

To our knowledge, this formulation for the jumping probability density function is new. The case of central concern in simulations is when the random walker begins at the origin, $w(\mathbf{r}=\mathbf{0},\mathbf{r}_B)$. Hereafter, we will denote this special density function by simply suppressing the argument $\mathbf{r}=\mathbf{0}$, i.e.,

$$w(\mathbf{r}_B) \equiv w(\mathbf{r}=\mathbf{0},\mathbf{r}_B). \tag{2.17}$$

Finally, another important quantity is the jumping probability $p(\mathbf{r})$ which gives the probability that the random walker, starting at $\mathbf{r}$, arrives on a certain portion of the first-passage surface $\partial\Omega_0$ for the first time. This is obtained by integrating the density function $w(\mathbf{r},\mathbf{r}_B)$ over boundary points on $\partial\Omega_0$, i.e.,

$$p(\mathbf{r}) = \int_{\partial\Omega_0} w(\mathbf{r},\mathbf{r}_B)d\mathbf{r}_B. \tag{2.18}$$

Using this expression and relations (2.15)–(2.16), yields the appropriate boundary-value problem for the jumping probability $p(\mathbf{r})$:

$$\nabla^2 p(\mathbf{r}) = 0, \quad \mathbf{r} \text{ in } \Omega, \tag{2.19}$$

subject to the boundary condition

$$p(\mathbf{r}) = \begin{cases} 1, & \mathbf{r} \text{ on } \partial\Omega_0,\\ 0, & \mathbf{r} \text{ not on } \partial\Omega_0.\end{cases} \tag{2.20}$$

To summarize, the three quantities of central concern for Brownian motion simulations are the mean hitting time $\tau(\mathbf{r})$, jumping probability density function $w(\mathbf{r},\mathbf{r}_B)$, and jumping probability $p(\mathbf{r})$. All of these quantities are obtained by solving steady-state diffusion equations: $\tau(\mathbf{r})$ is found from Eqs. (2.12) and (2.13), and $w(\mathbf{r},\mathbf{r}_B)$ is found from Eqs. (2.15) and (2.16), and $p(\mathbf{r})$ is found from Eqs. (2.19) and (2.20).

B. Heterogeneous situation

Let us now consider a two-phase, d-dimensional heterogeneous medium of conductivities σ_1 and σ_2. We will now develop the appropriate first-passage time formulation of this problem. The heterogeneous formulation is similar to the homogeneous one except for the important difference that interface continuity conditions must be satisfied. Since the steady-state formulation is easier to apply than the time-dependent one, we will only state the former explicitly. The time-dependent formalism for heterogeneous media follows from the homogeneous one in the obvious way.[13]

Consider a Brownian particle in the vicinity of the two-phase interface. At this instant of time, let us surround the particle with a *first-passage region* Ω having a bounding surface $\partial\Omega$ that encompasses both phases. Let Ω_i denote the portion of Ω containing phase i ($=1,2$) and $\partial\Omega_i$ denote the corresponding surface of Ω_i. Moreover, denote by Γ the interface surface. The mean hitting time satisfies the steady-state diffusion equation

$$\sigma_i\nabla^2\tau(\mathbf{r}) = -1, \quad \mathbf{r} \text{ in } \Omega_i, \tag{2.21}$$

subject to the absorbing boundary condition

$$\tau(\mathbf{r}) = 0, \quad \mathbf{r} \text{ on } \partial\Omega, \tag{2.22}$$

and the interface conditions

$$\tau|_1=\tau|_2, \quad \mathbf{r} \text{ on } \Gamma, \tag{2.23}$$

$$\left.\frac{\partial\tau}{\partial n_1}\right|_1=\frac{\sigma_2}{\sigma_1}\left.\frac{\partial\tau}{\partial n_1}\right|_2, \quad \mathbf{r} \text{ on } \Gamma, \tag{2.24}$$

where n_i is the unit outward normal from the region Ω_i and $|_i$ means the approach to Γ from the region Ω_i. Such equations describing the mean hitting time for heterogeneous media were first given by Kim and Torquato[10] for the case of a spherical first-passage sphere in d dimensions.

The jumping probability density function $w(\mathbf{r},\mathbf{r}_B)$ satisfies the steady-state diffusion equation

$$\nabla^2 w(\mathbf{r},\mathbf{r}_B)=0, \quad \mathbf{r} \text{ in } \Omega, \tag{2.25}$$

subject to the boundary condition

$$w=\delta(\mathbf{r}-\mathbf{r}_B), \quad \mathbf{r} \text{ on } \partial\Omega, \tag{2.26}$$

and the interface conditions

$$w|_1=w|_2, \quad \mathbf{r} \text{ on } \Gamma, \tag{2.27}$$

$$\left.\frac{\partial w}{\partial n_1}\right|_1=\frac{\sigma_2}{\sigma_1}\left.\frac{\partial w}{\partial n_1}\right|_2, \quad \mathbf{r} \text{ on } \Gamma. \tag{2.28}$$

To our knowledge, Eqs. (2.25)–(2.28) are new.

The probability $p_1(\mathbf{r})$ $[p_2(\mathbf{r})]$ that the random walker, initially at $\mathbf{r}$, hits the first-passage surface $\partial\Omega_1$ $[\partial\Omega_2]$ for the first time is found by integrating the above density function $w(\mathbf{r},\mathbf{r}_B)$ over boundary points on $\partial\Omega_1$, i.e.,

$$p_1(\mathbf{r})=\int_{\partial\Omega_1} w(\mathbf{r},\mathbf{r}_B)d\mathbf{r}_B. \tag{2.29}$$

Using this expression and relations (2.25)–(2.28), yields the appropriate boundary-value problem for the jumping probability $p_1(\mathbf{r})$:

$$\nabla^2 p_1(\mathbf{r})=0, \quad \mathbf{r} \text{ in } \Omega, \tag{2.30}$$

subject to the boundary condition

$$p_1(\mathbf{r})=\begin{cases}1, & \mathbf{r} \text{ on } \partial\Omega_1,\\ 0, & \mathbf{r} \text{ on } \partial\Omega_2.\end{cases} \tag{2.31}$$

and the interface conditions

$$p|_1=p|_2, \quad \mathbf{r} \text{ on } \Gamma, \tag{2.32}$$

$$\left.\frac{\partial p}{\partial n_1}\right|_1=\frac{\sigma_2}{\sigma_1}\left.\frac{\partial p}{\partial n_1}\right|_2, \quad \mathbf{r} \text{ on } \Gamma. \tag{2.33}$$

Once $p_1(\mathbf{r})$ is known, the jumping probability $p_2(\mathbf{r})$ for a point on the surface containing phase 2, $\partial\Omega_2$, is obtained from the trivial relation

$$p_2(\mathbf{r})=1-p_1(\mathbf{r}). \tag{2.34}$$

The expressions (2.30)–(2.34) for the jumping probabilities were first introduced and solved by Kim and Torquato[9] for first-passage spheres.

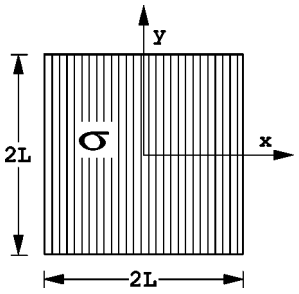

FIG. 1. First-passage square containing an homogeneous phase of conductivity σ.

III. FIRST-PASSAGE-TIME EQUATIONS FOR DIGITIZED MEDIA

We solve the appropriate diffusion equations to get the first-passage-time quantities τ, w, and p in the homogeneous and heterogeneous situations for square-shaped and cubical first-passage regions. The former and latter are applicable to two- and three-dimensional digitized media.

A. Two-dimensional digitized media

1. Homogeneous situation

Consider a first-passage square with a side of length $2L$ in an homogeneous medium of conductivity σ. The origin of the coordinate system is taken to be the center of the square, as depicted in Fig. 1. Let the Cartesian components of the walker position $\mathbf{r}$ be x and y. The mean hitting time $\tau(\mathbf{r})$ that solves Eqs. (2.12) and (2.13) is easily obtained using the separation of variables technique. The mean hitting time τ for a walk starting at the origin is found by evaluating this solution at $\mathbf{r}=\mathbf{0}$, yielding the analytical expression

$$\tau=\frac{L^2}{2\sigma}-\frac{16L^2}{\sigma\pi^3}\sum_{n=0}^{\infty}\frac{(-1)^n}{(2n+1)^3\cosh[(2n+1)\pi/2]}. \tag{3.1}$$

The series of Eq. (3.1) for τ can be summed numerically to yield

$$\tau\approx\frac{0.295L^2}{\sigma}. \tag{3.2}$$

Siegel and Langer[7] used this expression to simulate *homogeneous* diffusion in constricted two-dimensional pore geometries. It should be noted that they never considered walkers in heterogeneous media.

To compute the jumping probability density function, we will select boundary points y_B along the side $x=L$. In accordance with relations (2.15) and (2.16), we must solve the following boundary-value problem for the jumping probability density $w(x,y)$ for the homogeneous situation:

$$\frac{\partial^2 w}{\partial x^2}+\frac{\partial^2 w}{\partial y^2}=0, \quad -L\leqslant x\leqslant L, \quad L\leqslant y\leqslant L, \tag{3.3}$$

$$w(-L,y)=w(x,-L)=w(x,L)=0, \tag{3.4}$$

$$w(L,y)=\delta(y-y_B). \tag{3.5}$$

The solution of this boundary-value problem is readily obtained using the separation of variables technique, with the result that

$$w(x,y,y_B)=\frac{1}{L}\sum_{n=1}^{\infty}\frac{\sinh\left[\frac{n\pi}{2L}(x+L)\right]\sin\left[\frac{n\pi}{2L}(y+L)\right]\sin\left[\frac{n\pi}{2L}(y_B+L)\right]}{\sinh[n\pi]}. \tag{3.6}$$

Our interest is in the case when the random walker starts at the center of the square and hence we need the solution

$$w(y_B)\equiv w(0,0,y_B)=\frac{1}{2L}\sum_{n=1}^{\infty}\frac{\sin\left[\frac{n\pi}{2}\right]\sin\left[\frac{n\pi}{2L}(y_B+L)\right]}{\cosh\left[\frac{n\pi}{2}\right]}. \tag{3.7}$$

This jumping density function is plotted in Fig. 2. The probability that the random walker land for the first time at any point along the side $x=L$ is obtained by integrating Eq. (3.7) over all y_B, i.e.,

$$p=\int_{-L}^{L}w(y_B)dy_B=\frac{1}{4}. \tag{3.8}$$

Not surprisingly, for an homogeneous first-passage square, this probability is 1/4. Indeed, the jumping density function $w(y_B)$ for any side of the square takes the form of Eq. (3.7) and the probability to jump to any side is 1/4. Of course, this will not be true of heterogeneous media, as we shall see below.

2. Heterogeneous situation

Consider a first-passage square with a side of length $2L$ encompassing a walker that is in the vicinity of the two-phase interface. Again, the origin of the coordinate system is taken to be the center of the square. The first-passage square contains exactly four pixels that may be of phase 1 or 2 (each pixel having side of length L). Figure 3 depicts four possible phase configurations within the first-passage square. Let us first consider case (a). The mean hitting time $\tau(\mathbf{r})$ that solves Eqs. (2.21) and (2.24) is again obtained using the separation of variables technique. Evaluating this expression at $\mathbf{r}=\mathbf{0}$ gives the exact result

$$\tau=\frac{2}{\sigma_1+\sigma_2}\tau_H, \tag{3.9}$$

where τ_H denotes the homogeneous solution given by Eq. (3.1) for a *unit conductivity*. (Kim and Torquato[10] showed that precisely the same equation applies to a first-passage circle centered on the interface, given that the walker starts at the center.) It is easily shown that Eq. (3.9) applies to the situation (b). In the case (c), we have that

$$\tau=\frac{4}{3\sigma_1+\sigma_2}\tau_H. \tag{3.10}$$

More generally, if $\sigma^{(i)}$ designates the conductivity contained in the ith quadrant [see Fig. 3(d)], then we find that

$$\tau=\frac{1}{\overline{\sigma}}\tau_H, \tag{3.11}$$

where

$$\overline{\sigma}=\frac{1}{4}\sum_{i=1}^{4}\sigma^{(i)} \tag{3.12}$$

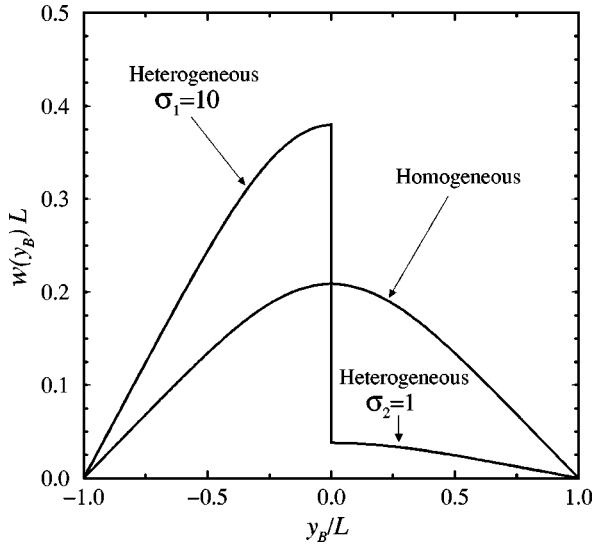

FIG. 2. Jumping probability density function $w(y_B)$ vs y_B for the side $x=L$ for an homogeneous situation, as well as the heterogeneous case (a) of Fig. 3.

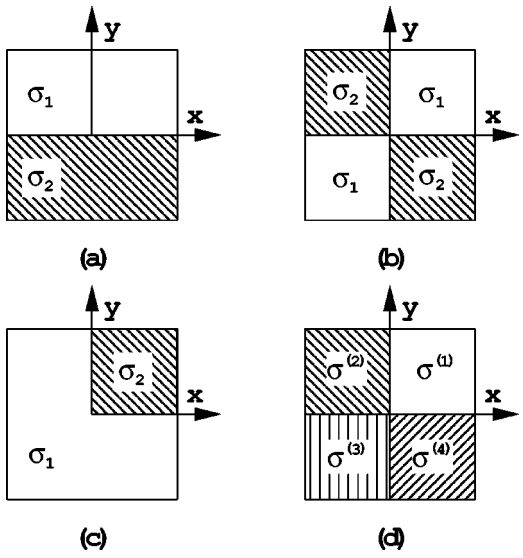

FIG. 3. First-passage square containing different phase conductivities. Four different cases are shown: (a), (b), (c), and the general situation (d).

is just the average conductivity in the first-passage square. It is important to note that formula (3.11) applies generally to multiphase media, i.e., composites with arbitrary number of phase conductivities.

Now we obtain the jumping probability density function $w(x,y)$ for case (a). According to Eqs. (2.25)–(2.28), we must solve the following boundary-value problem for $w(x,y)$:

$$\frac{\partial^2 w}{\partial x^2}+\frac{\partial^2 w}{\partial y^2}=0, \quad -L\leqslant x\leqslant L, \quad -L\leqslant y\leqslant L, \tag{3.13}$$

$$w(-L,y)=w(x,-L)=w(x,L)=0, \tag{3.14}$$

$$w(L,y)=\delta(y-y_B), \tag{3.15}$$

$$w(x,y)|_1=w(x,y)|_2, \tag{3.16}$$

$$\left.\frac{\partial w(x,y)}{\partial y}\right|_1=\frac{\sigma_2}{\sigma_1}\left.\frac{\partial w(x,y)}{\partial y}\right|_2. \tag{3.17}$$

This boundary-value problem is solved in the Appendix. Of particular interest is the solution at the origin, namely,

$$w(y_B)\equiv w(0,0,y_B)=\begin{cases}\dfrac{2\sigma_2}{\sigma_1+\sigma_2}w_H(y_B), & -L\leqslant y_B<0,\\ \dfrac{2\sigma_1}{\sigma_1+\sigma_2}w_H(y_B), & 0<y_B\leqslant L,\end{cases} \tag{3.18}$$

where $w_H(y_B)$ is the homogeneous solution given by Eq. (3.7). A plot of the heterogeneous solution $w(y_B)$ is included in Fig. 2. It is seen that $w_H(y_B)$ is discontinuous at $y_B=0$. The probability p that the random walker land for the first time along the side $x=L$ is given by

$$p=\int_{-L}^{L}w(y_B)dy_B=\frac{\sigma_2}{4(\sigma_1+\sigma_2)}+\frac{\sigma_1}{4(\sigma_1+\sigma_2)}=\frac{1}{4}. \tag{3.19}$$

Notice that each phase region contributes differently to p but together sum to 1/4. Observe that if we consider instead the boundary points y_B on the side $x=-L$, we get the identical result of Eq. (3.18) for the density function.

If we consider boundary points x_B on the side $y=L$, we find that $w(x_B)$ is a continuous function given by

$$w(x_B)=\frac{2\sigma_1}{\sigma_1+\sigma_2}w_H(x_B), \quad -L\leqslant x_B\leqslant L. \tag{3.20}$$

The probability p that the random walker land for the first time at any point along the side $y=L$ is given by

$$p=\int_{-L}^{L}w(x_B)dx_B=\frac{\sigma_1}{2(\sigma_1+\sigma_2)}. \tag{3.21}$$

If we consider boundary points x_B on the side $y=-L$, we find that $w(x_B)$ is a continuous function given by

$$w(x_B)=\frac{2\sigma_2}{\sigma_1+\sigma_2}w_H(x_B), \quad -L\leqslant x_B\leqslant L. \tag{3.22}$$

The probability p that the random walker land for the first time at any point along the side $y=L$ is given by

$$p=\int_{-L}^{L}w(x_B)dx_B=\frac{\sigma_2}{2(\sigma_1+\sigma_2)}. \tag{3.23}$$

More generally, the density function w is obtainable for the most general situation given by case (d) in Fig. 3. Let q_B represent the boundary coordinate on any side of the first-passage square. Then the general expression is given by

$$w(q_B)=\begin{cases}\dfrac{\sigma^{(i)}(q_B)}{\overline{\sigma}}w_H(q_B), & -L\leqslant q_B<0,\\ \dfrac{\sigma^{(i)}(q_B)}{\overline{\sigma}}w_H(q_B), & 0<q_B\leqslant L,\end{cases} \tag{3.24}$$

where $\sigma^{(i)}(q_B)$ is the *constant* conductivity of the ith quadrant, which depends on the boundary coordinate q_B, and $\overline{\sigma}$ is given by Eq. (3.12). It is important to realize that $\sigma^{(i)}(q_B)$ is generally piecewise constant: it is constant in the interval $[-L,0)$ and generally another constant in $(0,L]$. Integrating Eq. (3.24) over q_B gives the corresponding jumping probability p for this side:

$$p=\frac{\sigma^{(i)}(q_B)}{8\overline{\sigma}}+\frac{\sigma^{(j)}(q_B)}{8\overline{\sigma}}, \tag{3.25}$$

where $i\neq j$ denote the quadrant numbers that share an edge of the first-passage square $[(i,j)=\{(1,2),(1,4),(2,3),(3,4)\}]$.

B. Three-dimensional digitized media

1. Homogeneous situation

Here we formulate the appropriate first-passage-time equations for a cubical first-passage region. Since the solutions follow closely the two-dimensional case of squares, we do not give the same level of detail as in the former.

Consider a first-passage cube with a side of length $2L$. The origin of the coordinate system is taken to be the center

of the cube. Let the Cartesian components of the walker position $\mathbf{r}$ be x, y, and z. Using the separation of variables technique, the mean hitting time $\tau(\mathbf{r})$ that solves Eqs. (2.12) and (2.13) is easily obtained. The mean hitting time τ for a walk starting at the origin is found by evaluating this solution at $\mathbf{r}=\mathbf{0}$, giving

$$\tau=\frac{L^2}{2\sigma}-\frac{16L^2}{\sigma\pi^3}\sum_{m=0}^{\infty}\frac{(-1)^m}{\gamma^3(m)\cosh\left[\gamma(m)\frac{\pi}{2}\right]}-\frac{64L^2}{\sigma\pi^4}\sum_{m,n=0}^{\infty}\frac{(-1)^m(-1)^n}{\gamma(m)\gamma(n)\theta^2\cosh\left[\theta\frac{\pi}{2}\right]}, \tag{3.26}$$

where

$$\gamma(n)=2n+1 \quad \text{and} \quad \theta^2=\gamma^2(m)+\gamma^2(n). \tag{3.27}$$

The series of Eq. (3.26) for τ can be summed numerically to give

$$\tau\approx\frac{0.22485L^2}{\sigma}. \tag{3.28}$$

Coker and Torquato[14] used this expression to study diffusion-controlled reactions in three-dimensional digitized media.

The jumping probability density function $w(x,y,z,y_B,z_B)$ is calculated for boundary coordinates (y_B,z_B) along the face $x=L$. We must solve the differential Eq. (2.15) boundary-value subject to the boundary conditions that each face the density is zero, except at the face $x=L$, where $w(L,y,z)=\delta(y-y_B)\delta(z-z_B)$. The solution of this boundary-value problem is obtained using the separation of variables technique. Our interest is in the case when the random walker starts at the center of the square and hence we need the solution $w(y_B,z_B)\equiv w(0,0,0,y_B,z_B)$ given by

$$w(y_B,z_B)=\frac{1}{2L^2}\sum_{m=1}^{\infty}\sum_{n=1}^{\infty}\frac{\sin\left[\frac{m\pi}{2}\right]\sin\left[\frac{m\pi}{2L}(y_B+L)\right]\sin\left[\frac{n\pi}{2}\right]\sin\left[\frac{n\pi}{2L}(z_B+L)\right]}{\cosh[kL]}, \tag{3.29}$$

where

$$k^2=\left(\frac{\pi}{2L}\right)^2(m^2+n^2), \tag{3.30}$$

for any integer m or n.

The probability that the random walker land for the first time at any point on the face $x=L$ is obtained by integrating Eq. (3.29) over all y_B and z_B, i.e.,

$$p=\int_{-L}^{L}\int_{-L}^{L}w(y_B,z_B)dy_Bdz_B=\frac{1}{6}. \tag{3.31}$$

As expected, for an homogeneous first-passage cube, this probability is 1/6. Indeed, the jumping density function $w(y_B,z_B)$ for any side of the square takes the form of Eq. (3.29) and the probability to jump to any side is 1/6. This will not be true of heterogeneous media, as we shall see below.

2. Heterogeneous situation

Consider a first-passage cube with a side of length $2L$ encompassing a walker that is in the vicinity of the two-phase interface. The origin of the coordinate system is taken to be the center of the square. The first-passage square contains exactly eight voxels that may be of phase 1 or 2 (each voxel having side of length L). We will immediately consider the three-dimensional analog of the two-dimensional case (d) of Fig. 3, i.e., the ith octant has a conductivity $\sigma^{(i)}$. The mean hitting time $\tau(\mathbf{r})$ that solves Eqs. (2.21) and (2.24) is found using the separation of variables technique. In particular, at $\mathbf{r}=\mathbf{0}$ it is found that

$$\tau=\frac{1}{\overline{\sigma}}\tau_H, \tag{3.32}$$

where

$$\overline{\sigma}=\frac{1}{8}\sum_{i=1}^{8}\sigma^{(i)} \tag{3.33}$$

is the average conductivity in the first-passage cube.

The corresponding jumping probability density function $w(x,y,z)$ for this case requires us to solve Eqs. (2.25)–(2.28). We find that for any face of the cube, where (q_B,p_B) represents the boundary point on this face, that

$$w(q_B,p_B)=\begin{cases}\dfrac{\sigma^{(i)}(q_B,p_B)}{\overline{\sigma}}w_H(q_B,p_B), & -L\leqslant q_B<0,\ -L\leqslant p_B<0,\\ \dfrac{\sigma^{(i)}(q_B,p_B)}{\overline{\sigma}}w_H(q_B,p_B), & -L\leqslant q_B<0,\ 0<p_B\leqslant L,\\ \dfrac{\sigma^{(i)}(q_B,p_B)}{\overline{\sigma}}w_H(q_B,p_B), & 0<q_B\leqslant L,\ -L\leqslant p_B<0,\\ \dfrac{\sigma^{(i)}(q_B,p_B)}{\overline{\sigma}}w_H(q_B,p_B), & 0<q_B\leqslant L,\ 0<p_B\leqslant L,\end{cases} \tag{3.34}$$

where $\sigma^{(i)}(q_B,p_B)$ is the *constant* conductivity of the ith octant, which depends on the boundary coordinate q_B,p_B, and $\overline{\sigma}$ is given by Eq. (3.33). Integrating Eq. (3.34) over q_B and p_B gives the corresponding jumping probability p for this face:

$$p=\frac{\sigma^{(i)}(q_B,p_B)}{24\overline{\sigma}}+\frac{\sigma^{(j)}(q_B,p_B)}{24\overline{\sigma}}+\frac{\sigma^{(k)}(q_B,p_B)}{24\overline{\sigma}}+\frac{\sigma^{(l)}(q_B,p_B)}{24\overline{\sigma}}, \tag{3.35}$$

where $i\neq j\neq k\neq l$ denote the octant numbers that share a face of the first-passage cube [see formula (3.25) for two dimensions].

IV. SIMULATION DETAILS FOR DIGITIZED MEDIA

The basic idea of the first-passage-time algorithm to compute the effective conductivity of digitized composites is similar to the one discussed in the Introduction that utilizes first-passage spheres. One must release many random walkers (i.e., conduction tracers) to sample the medium. The effective conductivity is obtained from the slope of the mean-square displacement versus time at sufficiently long times. However, there are some simulation details that are different in the case of digitized composites, which we describe below in the language of two dimensions for concreteness. Given this discussion, the extension to three dimensions is obvious.

For a given digitized medium, a random walker begins its travel from a randomly chosen point inside the medium. In order to move to another location, a first-passage square is constructed about the random walker. The first-passage square lies in either an homogeneous or heterogeneous region, depending on whether the random walker happens to be at the interface boundary or not.

A. Homogeneous situation

For most times, a random walker will be located away from the interface boundary. In such cases, an homogeneous first-passage square is constructed such that it is centered at the position of the walker and its size is maximized while remaining homogeneous (purely phase 1 or 2). Constructing the first-passage square this way guarantees that at least one of its four sides touches the interface boundary. Once the first-passage square is constructed, the random walker then jumps onto an arbitrary location at the boundary of this first-passage square (not to be confused with the interface boundary). This is done by first selecting the side. The specific boundary point where the random walker jumps to is determined by the probability density function $w(\mathbf{r},\mathbf{r}_B)$ given by Eq. (3.7).[15] Furthermore, this jump takes an amount of time τ_H, given by Eq. (3.1), for a first-passage square of length $2L$ in a medium of conductivity σ_i. (Note that the size of the first-passage square is generally not limited to discrete multiples of the pixel size, i.e., L can take on a continuous range of values.) For each movement within this homogeneous region, a first-passage square is constructed, τ_H is recorded, and the process is repeated until the random walker eventually lands exactly on the interface boundary. For further movement of the random walker, a first-passage square has to be constructed that encompasses both phases.

B. Heterogeneous situation

When the random walker is at the interface boundary, a heterogeneous first-passage square is constructed for the walker's next move. It can be either at the interface boundary between two neighboring pixels (off the corner) or at the interface boundary among four neighboring pixels (on the corner). Note that every interface boundary should be at pixel boundaries. If the random walker is at the interface boundary between two pixels of different phases, the heterogeneous first-passage square is constructed such that it is centered at the position of the walker and one of its four sides includes the nearest corner (four-pixel boundary). The *shape* of the resulting heterogeneous first passage square will be as shown in Fig. 3(a); however, note that the first-passage square in this case will be smaller than a pixel. If the random walker is within some very small distance δ (equal to 10^{-8} of a pixel size) of a pixel corner which is locally heterogeneous, the walker is placed exactly on the corner and an heterogeneous first-passage square, exactly four times as large as a pixel, is constructed that is centered on the walker.[16] Some possible resulting heterogeneous first-passage squares will be as shown in (a), (b), or (c) of Fig. 3. For the case shown in Fig. 3(b), the corner appears as a *choked neck* to the random walker at more conducting phase. For example, if the white region in Fig. 3(b) is less conducting and hence the walker is less active in this region, the walker has to get through the corner from a shaded region to the opposite shaded region to yield the long-time behavior. Whether the walker is at the two-pixel boundary or the four-

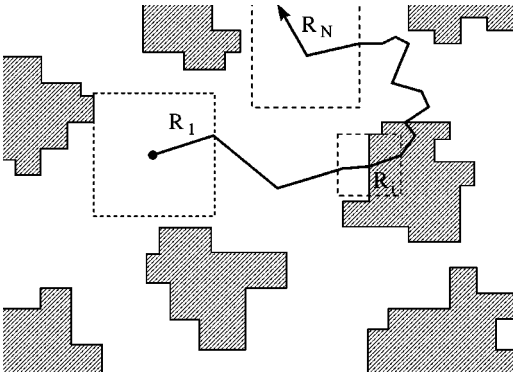

FIG. 4. A random walker makes an initial jump of distance R_1 to the boundary of the first-passage square. It crosses the two-phase interface for the first time in the ith jump and reaches sample boundary at the Nth jump.

pixel boundary, once the heterogeneous first-passage square is constructed, the walker then jumps to an arbitrary point on the boundary of the first-passage square. This is done by first selecting the side according to the probability specified by Eq. (3.25). The specific boundary point where the random walker jumps to is determined by the probability density function $w(q_B)$ given by Eq. (3.24). The amount of time τ taken for this jump is given by Eq. (3.11). For each movement utilizing an heterogeneous first-passage square, τ is recorded and the process is repeated whenever the random walker lands at the interface boundary.

By repeated use of homogeneous or heterogeneous first-passage squares (see Fig. 4), the random walker can continue to travel as long as needed. After a sufficiently long time, another random walker begins its travel from another randomly chosen point in the medium. Averaging over sufficiently many random walkers, one can obtain the effective conductivity σ_e given by Eq. (1.1) for a particular configuration of the digitized medium. For disordered media, one must average over sufficiently many configurations.

V. RESULTS FOR PERIODIC AND RANDOM CHECKERBOARDS

A. Periodic checkerboard

A severe test of the algorithm is the task of finding the effective conductivity σ_e of the two-dimensional periodic checkerboard (see Fig. 5) for moderate to high phase contrasts. By definition the phase volume fractions are equal, i.e., $\phi_1=\phi_2=0.5$, where ϕ_i is the volume fraction of phase i. It is well known that the effective conductivity of such a microgeometry is given exactly for any phase contrast by the expression[17]

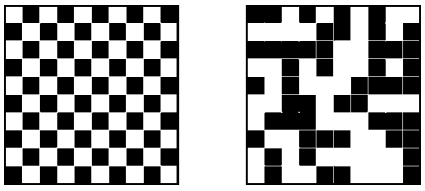

FIG. 5. (a) Portion of a periodic checkerboard in which $\phi_1=\phi_2=0.5$, by definition. (b) Portion of a random checkerboard in which $\phi_1=\phi_2=0.5$.

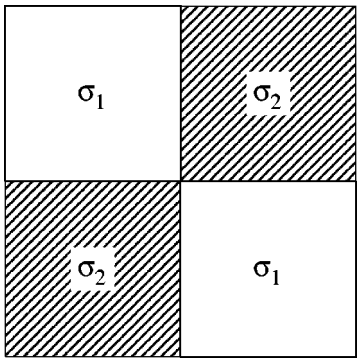

FIG. 6. Periodic unit cell used in finite difference calculation for periodic checkerboard.

$$\sigma_e=\sqrt{\sigma_1\sigma_2}. \tag{5.1}$$

When one phase (say phase 1) is appreciably more conducting than the other (phase 2), most of the current must pass through the corner contact points of phase 1. That is, such corner regions are characterized by high field concentrations.

As noted in the Introduction, it is difficult for conventional finite difference or finite element techniques to capture accurately the local fields in such situations with a reasonable grid resolution. We carried out a finite difference calculation to find σ_e for the regular checkerboard with a unit cell depicted in Fig. 6 for various values of the grid resolution N when $\sigma_1/\sigma_2=100$. A value of $N=2$ corresponds to a grid as large as the smallest square element in the system. Our results are summarized in Fig. 7 where we give a log-log plot of the effective conductivity versus resolution N. It seen that even when $N=256$, the effective conductivity is predicted to be 6.896, which is significantly below the exact result of 10. Moreover, the approach to the exact value with increasing N is quite slow.

The deficiencies of the finite difference method here are to be contrasted with our Brownian motion method for digi-

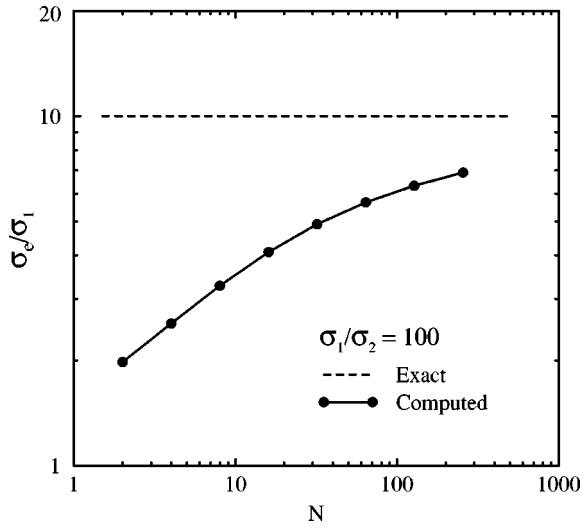

FIG. 7. Log-log plot of scaled effective conductivity σ_e/σ_1 vs resolution N used in finite-difference computation for the periodic checkerboard when $\sigma_1/\sigma_2=100$. The exact result of 10 is also shown.

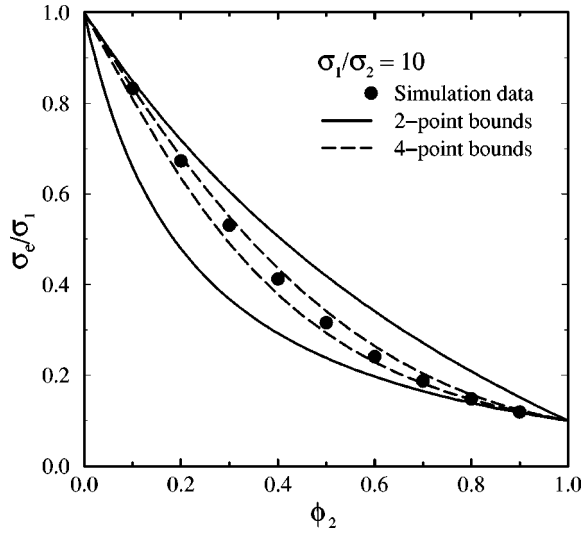

FIG. 8. Our Brownian motion simulation data for the effective conductivity σ_e vs phase 2 volume fraction ϕ_2 for the random checkerboard when $\sigma_1/\sigma_2=10$. Included are the two- and four-point bounds.

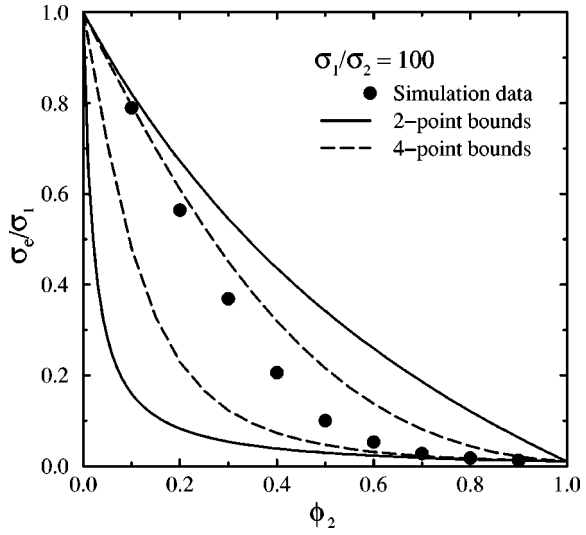

FIG. 9. Our Brownian motion simulation data for the effective conductivity σ_e vs phase 2 volume fraction ϕ_2 for the random checkerboard when $\sigma_1/\sigma_2=100$. Included are the two- and four-point bounds.

tized media which yields an effective conductivity $\sigma_e=10.063$ for the regular checkerboard when $\sigma_1/\sigma_2=100$. This result is obtained by averaging over 10^6 random walkers.

B. Random checkerboard

We have also applied the algorithm to compute the effective conductivity of the random checkerboard. The random checkerboard is generated by tessellating two-dimensional space into a square lattice and assigning to each square phase i according to the probability ϕ_i (see Fig. 5). We note that this is a special case of a symmetric-cell material,[18] i.e., one with square cells. Observe also that for nearest-neighbor connections, the percolation threshold of the random checkerboard corresponds to the occupied site percolation value of approximately 0.592.[19]

We have computed the effective conductivity of the random checkerboard for a wide range of volume fractions and for two phase contrast ratios: $\sigma_1/\sigma_2=10$ and $\sigma_1/\sigma_2=100$. Our simulation results are summarized in Figs. 8 and 9. We studied systems up to 1000×1000 in size and examined 100 different configurations. We employed up to 5000 random walks for each volume fraction. Note that the effective conductivities for the corresponding reciprocal cases $\sigma_1/\sigma_2=0.1$ and $\sigma_1/\sigma_2=0.01$ are immediately obtainable from the data in Figs. 8 and 9 and the phase-interchange theorem[20] for two-dimensional, two-phase, isotropic composite media given by

$$\sigma_e(\sigma_1,\sigma_2)\sigma_e(\sigma_2,\sigma_1)=\sigma_1\sigma_2, \tag{5.2}$$

where $\sigma_e(\sigma_2,\sigma_1)$ is the effective conductivity for a composite in which the phases are interchanged.

Our results are compared to two sets of rigorous bounds on the effective conductivity. The first set of bounds that we employ are the two-point Hashin–Shtrikman bounds[21] which, for $\sigma_1\geqslant\sigma_2$, are given by

$$\sigma_e^{(2L)}\leqslant\sigma_e\leqslant\sigma_e^{(2U)}, \tag{5.3}$$

where

$$\sigma_e^{(2U)}=\langle\sigma\rangle-\frac{\phi_1\phi_2(\sigma_1-\sigma_2)^2}{\langle\tilde{\sigma}\rangle+\sigma_1},$$
$$\sigma_e^{(2L)}=\langle\sigma\rangle-\frac{\phi_1\phi_2(\sigma_1-\sigma_2)^2}{\langle\tilde{\sigma}\rangle+\sigma_2}, \tag{5.4}$$

$$\langle\sigma\rangle=\phi_1\sigma_1+\phi_2\sigma_2,\quad \langle\tilde{\sigma}\rangle=\phi_1\sigma_2+\phi_2\sigma_1. \tag{5.5}$$

These are referred to as two-point bounds since they incorporate up to two-point correlation function information about the microstructure.[5] The bounds are exact through second order in the difference in the phase conductivities.

We also make use of the sharper four-point Milton bounds[22] which, for $\sigma_1\geqslant\sigma_2$, are given by

$$\sigma_e^{(4L)}\leqslant\sigma_e\leqslant\sigma_e^{(4U)}, \tag{5.6}$$

where

$$\sigma_e^{(4U)}=\langle\sigma\rangle-\frac{\phi_1\phi_2(\sigma_1-\sigma_2)^2}{\langle\tilde{\sigma}\rangle+y_1},$$
$$\sigma_e^{(4L)}=\langle\sigma\rangle-\frac{\phi_1\phi_2(\sigma_1-\sigma_2)^2}{\langle\tilde{\sigma}\rangle+y_2}, \tag{5.7}$$

$$y_1=\frac{\sigma_2(\sigma_1+\langle\sigma\rangle_\zeta)}{\sigma_2+\langle\tilde{\sigma}\rangle_\zeta},\quad y_2=\frac{\sigma_1(\sigma_2+\langle\sigma\rangle_\zeta)}{\sigma_1+\langle\tilde{\sigma}\rangle_\zeta}, \tag{5.8}$$

$$\langle\sigma\rangle_\zeta=\sigma_1\zeta_1+\sigma_2\zeta_2,\quad \langle\tilde{\sigma}\rangle_\zeta=\sigma_1\zeta_2+\sigma_2\zeta_1. \tag{5.9}$$

The quantities ζ_1 and $\zeta_2=1-\zeta_1$ are microstructural parameters that depends on three-point correlation function information. However, even though only ζ_i appears, the bounds actually depend on four-point information, which in the spe-

cial case of two dimensions, can be expressed in terms of ζ_1 or ζ_2. These bounds are exact through fourth order in the difference in the phase conductivities.

One can compute ζ_2 for the random checkerboard by utilizing a technique used by Torquato[23] for another microgeometry. Specifically, by comparing the aforementioned perturbation expansion to the recent low-concentration results of Hetherington and Thorpe[24] for square inclusions (expanded in powers of the difference in the phase conductivities), we find

$$\zeta_2 = 0.08079 + 0.83842\phi_2. \tag{5.10}$$

The two- and four-point bounds are included in Figs. 8 and 9. It is seen that for the moderate contrast $\sigma_1/\sigma_2 = 10$, the simulation data lie within the very tight four-point bounds. In the high-contrast case ($\sigma_1/\sigma_2 = 100$), the data lie closer to the upper bound for small volume fractions of the nonconducting phase (phase 2). Above the percolation threshold of the nonconducting phase (≈ 0.592), the data lie closer to the lower bound. Such behavior of the bounds well below and above the percolation threshold is well known.[5] As ϕ_2 increases for intermediate values, the data make a transition from being closer to the upper bound to being closer to the lower bound, as expected.

VI. CONCLUSIONS

The major results of this article are both theoretical and computational in nature. On the theoretical side, we have generalized the first-passage-time analysis of Kim and Torquato[9] to compute the effective conductivity, dielectric constant, and diffusion coefficient of digitized composite media. We accomplished this via the first-passage-time *canonical function* $P(\mathbf{r},\mathbf{r}_B,t)$ [defined by Eqs. (2.1)–(2.3)] for first-passage regions of arbitrary shape. From the canonical function, we showed how one can derive the three key first-passage-time quantities: mean hitting time $\tau(\mathbf{r})$, jumping probability density function $w(\mathbf{r},\mathbf{r}_B)$, and the jumping probability $p(\mathbf{r})$. From this formalism, we then derived the appropriate first-passage-time equations for digitized media: first-passage squares in two dimensions and first-passage cubes in three dimensions.

On the computational side, we then provided an algorithm to apply the first-passage-time equations to compute the effective conductivity of digitized composite media. In order to test the algorithm, we applied it to compute the effective conductivity of both the periodic and random checkerboards. The periodic checkerboard is a severe test case since conduction is dominated by corners that join two conducting-phase pixels at sufficiently large phase contrasts. Conventional numerical techniques (such as finite differences or elements) do not accurately capture the local fields here for reasonable grid resolution and hence lead to inaccurate estimates of the effective conductivity. By contrast, we have shown that our algorithm yields accurate estimates of the effective conductivity of the periodic checkerboard for widely different phase conductivities. We have computed the effective conductivity of the random checkerboard for a wide range of volume fractions and several phase contrast ratios. Our simulation results always lie within rigorous four-point bounds on the effective conductivity of the random checkerboard.

ACKNOWLEDGMENT

The authors gratefully acknowledge the support of the Office of Basic Energy Science, U.S. Department of Energy under Grant No. DE-FG02-92ER14275.

APPENDIX: PROBABILITY DENSITY FUNCTION FOR HETEROGENEOUS SITUATION

We solve the boundary-value problem of Eqs. (3.13)–(3.17) for the jumping probability density function $w(x,y)$ using the separation of variables technique. As in the homogeneous case, the x-dependent part of the solution will have the form

$$\sinh(\lambda_n x),$$

where λ_n are the eigenvalues for the problem to be determined below. The y-dependent part of the solution is given in terms of eigenfunctions of the form

$$A_n \sin(\lambda_n y) + B_n \cos(\lambda_n y),$$

where the A_n and B_n are unknown coefficients that depend on the value of the integer n. Application of the boundary conditions (3.14)–(3.17), yields a set of three equations that enables us to determine the coefficients A_n and B_n, as well as the eigenvalues $\lambda_n = n\pi/a$. After some algebra, the complete solution is easily obtained.

Now let us assume that the delta function is in phase 2 (i.e., $-L \leqslant y_B < 0$), then the density $w(x,y)$ that satisfies the boundary-value problem of Eqs. (3.13)–(3.17) is given by

$$w(x,y) = \begin{cases} \dfrac{2\sigma_2}{(\sigma_1+\sigma_2)L} \displaystyle\sum_{n=1}^{\infty} \dfrac{\sinh\left[\dfrac{n\pi}{2L}(x+L)\right]\sin\left[\dfrac{n\pi}{2L}(y+L)\right]\sin\left[\dfrac{n\pi}{2L}(y_B+L)\right]}{\sinh[n\pi]}, & 0 \leqslant y \leqslant L \\ \dfrac{2\sigma_2}{(\sigma_1+\sigma_2)L} \displaystyle\sum_{n=1}^{\infty} \dfrac{C_n \sinh\left[\dfrac{n\pi}{2L}(x+L)\right]\sin\left[\dfrac{n\pi}{2L}(y+L)\right]\sin\left[\dfrac{n\pi}{2L}(y_B+L)\right]}{\sinh[n\pi]}, & -L \leqslant y \leqslant 0 \end{cases}, \tag{A1}$$

where

$$C_n=\begin{cases}1, & \text{odd } n,\\ \sigma_1/\sigma_2, & \text{even } n.\end{cases} \tag{A2}$$

Our interest is in the case $x=y=0$ and hence

$$w(y_B)\equiv w(0,0,y_B)=\frac{2\sigma_2}{(\sigma_1+\sigma_2)L}\sum_{n=1}^{\infty}\frac{\sinh\left[\frac{n\pi}{2}\right]\sin\left[\frac{n\pi}{2}\right]\sin\left[\frac{n\pi}{2L}(y_B+L)\right]}{\sinh[n\pi]},\quad -L\leqslant y_B<0. \tag{A3}$$

Therefore,

$$w(y_B)=\frac{2\sigma_1}{\sigma_1+\sigma_2}w_H(y_B),\quad -L\leqslant y_B\leqslant 0, \tag{A4}$$

where $w_H(y_B)$ is the solution for the homogeneous situation of Eq. (3.7).

When $0<y_0\leqslant L$, then the density $w(x,y)$ is given by

$$w(x,y)=\begin{cases}\dfrac{2\sigma_1}{(\sigma_1+\sigma_2)L}\displaystyle\sum_{n=1}^{\infty}\dfrac{\sinh\left[\frac{n\pi}{2L}(x+L)\right]\sin\left[\frac{n\pi}{2L}(y+L)\right]\sin\left[\frac{n\pi}{2L}(y_B+L)\right]}{\sinh[n\pi]}, & 0\leqslant y\leqslant L\\ \dfrac{2\sigma_1}{(\sigma_1+\sigma_2)L}\displaystyle\sum_{n=1}^{\infty}\dfrac{C_n\sinh\left[\frac{n\pi}{2L}(x+L)\right]\sin\left[\frac{n\pi}{2L}(y+L)\right]\sin\left[\frac{n\pi}{2L}(y_B+L)\right]}{\sinh[n\pi]}, & -L\leqslant y<0\end{cases}. \tag{A5}$$

For the special case $x=y=0$, we have that

$$w(y_B)\equiv w(0,0,y_B)=\frac{2\sigma_1}{(\sigma_1+\sigma_2)L}\sum_{n=1}^{\infty}\frac{\sinh\left[\frac{n\pi}{2}\right]\sin\left[\frac{n\pi}{2}\right]\sin\left[\frac{n\pi}{2L}(y_B+L)\right]}{\sinh[n\pi]},\quad 0<y_B<L. \tag{A6}$$

We see that

$$w(y_B)=\frac{2\sigma_1}{\sigma_1+\sigma_2}w_H(y_B),\quad 0<y_B\leqslant L. \tag{A7}$$

[1] S. L. Flegler, *Scanning and Transmission Electron Microscopy: An Introduction* (W. H. Freeman, New York, 1993).
[2] J. A. Stroscio, *Scanning Tunneling Microscopy* (Academic, Boston, 1992).
[3] J. H. Kinney and M. C. Nichols, Annu. Rev. Mater. Sci. **22**, 121 (1992).
[4] J. T. Fredrich, B. Menendez, and T. F. Wong, Science **268**, 276 (1995).
[5] S. Torquato, Appl. Mech. Rev. **44**, 37 (1991).
[6] L. M. Schwartz and J. R. Banavar, Phys. Rev. B **39**, 11965 (1989).
[7] R. A. Siegel and R. Langer, J. Colloid Interface Sci. **109**, 426 (1986).
[8] S. Torquato and I. C. Kim, Appl. Phys. Lett. **55**, 1847 (1989).
[9] I. C. Kim and S. Torquato, J. Appl. Phys. **68**, 3892 (1990).
[10] I. C. Kim and S. Torquato, J. Appl. Phys. **69**, 2280 (1991); **71**, 2727 (1992).
[11] I. C. Kim and S. Torquato, J. Appl. Phys. **74**, 1844 (1993).
[12] L. Pontryagin, A. Andronow, and A. Wit, Zh. Eksp. Teor. Fiz. **3**, 172 (1933); S. Lifson and J. L. Jackson, J. Chem. Phys. **36**, 2410 (1962).
[13] Referring to the steady-state first-passage-time formulation for the heterogeneous situation, we see that the time-dependent formalism here for the canonical function $P(\mathbf{r},\mathbf{r}_B,t)$ follows closely the homogeneous one with the addition of the continuity conditions at the interface.
[14] D. A. Coker and S. Torquato, J. Appl. Phys. **77**, 955 (1995).
[15] As is standard practice, the associated cumulative distribution function is used to determine the location of the walker on the boundary.
[16] The assumption that the walker can be placed exactly at the corner when it is within some very small distance $\delta=10^{-8}$ of a pixel size introduces negligibly small error. Indeed, our experience shows that δ is actually sufficiently small if it is less than 10^{-6} times a pixel size.
[17] A. M. Dykhne, Sov. Phys. JETP **32**, 63 (1971).
[18] M. Miller, J. Math. Phys. **10**, 1988 (1969).
[19] D. Stauffer, *Introduction to Percolation Theory* (Taylor and Francis, London, 1986).
[20] J. B. Keller, J. Math. Phys. **5**, 548 (1964); K. S. Mendelson, J. Appl. Phys. **46**, 917 (1975).
[21] Z. Hashin, J. Mech. Phys. Solids **13**, 119 (1965).
[22] G. W. Milton, J. Appl. Phys. **52**, 5294 (1981).
[23] S. Torquato, J. Chem. Phys. **83**, 4776 (1985).
[24] J. Hetherington and M. F. Thorpe, Proc. R. Soc. London, Ser. A **438**, 591 (1992).